J|A|C|S ARTICLES

Published on Web 02/19/2010

In Situ Single-Crystal Diffraction Studies of the Structural Transition of Metal−Organic Framework Copper 5-Sulfoisophthalate, Cu-SIP-3

Phoebe K. Allan,[†] Bo Xiao,[†] Simon J. Teat,[‡] Jason W. Knight,[‡] and Russell E. Morris*,[†]

School of Chemistry, University of St. Andrews, North Haugh, St. Andrews, Fife KY16 9ST, Scotland, U.K., and Advanced Light Source, Lawrence Berkeley National Laboratories, Berkeley, California

Received December 16, 2009; E-mail: rem1@st-andrews.ac.uk

Abstract: The flexibility of the metal−organic framework $Cu_2(OH)(C_8H_3O_7S)(H_2O)\cdot 2H_2O$ (Cu-SIP-3) toward reversible single-crystal to single-crystal transformations is demonstrated using in situ diffraction methods at variable temperature. At temperatures below a dehydration-induced phase transition (T < 370 K) the structure is confirmed as being hydrated. In the temperature range where the transition takes place (370 K < T < 405 K) no discrete, sharp Bragg peaks can be seen in the single-crystal X-ray diffraction pattern, indicating significant loss of long-range order. At temperatures higher than 405 K, the Bragg peaks return and the structure can be refined as dehydrated Cu-SIP-3. The loss of guest water molecules can be followed at temperatures below the phase transition giving insight into the mechanism of the dehydration. Addition of nitric oxide gas to the material above the gating opening pressure of 275 mbar also leads to loss of Bragg scattering in the diffraction pattern.

Introduction

Metal−organic frameworks (MOFs, also known as porous coordination polymers) have attracted substantial attention in recent times due to their potential to address current technological issues in gas storage,[1−6] gas separation,[7−11] polymerization, and catalysis[11−16] applications. These materials consist of organic linkers connecting metals or metal clusters to form crystalline materials. A major advantage of MOFs is the very high surface areas which are achievable, greater than 5000 m^2 g^{-1} in the most porous materials, comparing favorably to that of zeolites, which is generally in the range of a few hundred m^2 g^{-1}. The flip side to this is the low thermal stability of many of the materials owing to the relatively weak metal−ligand interactions holding the materials together. However, there are now many framework materials reported that are stable after the removal of both solvent contained in framework channels and that coordinated to metal ions in the structure, leaving exposed metal sites which can enhance gas adsorption by interaction with the guest molecules.[17] Increasingly, there is a shift toward synthesizing more exotic frameworks, those which enhance gas adsorption or selectivity using interaction of guest molecules with framework features such as open polar organic linker substituents[18−20] or those frameworks which are flexible in response to an external stimulus such as heat or guest molecules.[21,22]

[†] University of St. Andrews.
[‡] Lawrence Berkeley National Laboratories.

(1) Dietzel, P. D. C.; Panella, B.; Hirscher, M.; Blom, R.; Fjellvag, H. *Chem. Commun.* **2006**, 959–961.
(2) Dinca, M.; Long, J. R. *J. Am. Chem. Soc.* **2007**, *129*, 11172–11176.
(3) Morris, R. E.; Wheatley, P. S. *Angew. Chem., Int. Ed.* **2008**, *47*, 4966–4981.
(4) Eddaoudi, M.; Kim, J.; Rosi, N.; Vodak, D.; Wachter, J.; O'Keeffe, M.; Yaghi, O. M. *Science* **2002**, *295*, 469–472.
(5) Rosi, N. L.; Eckert, J.; Eddaoudi, M.; Vodak, D. T.; Kim, J.; O'Keeffe, M.; Yaghi, O. M. *Science* **2003**, *300*, 1127–1129.
(6) Xue, M.; Liu, Y.; Schaffino, R. M.; Xiang, S. C.; Zhao, X. J.; Zhu, G. S.; Qiu, S. L.; Chen, B. L. *Inorg. Chem.* **2009**, *48*, 4649–4651.
(7) Bae, Y.-S.; Mulfort, K. L.; Frost, H.; Ryan, P.; Punnathanam, S.; Broadbelt, L. J.; Hupp, J. T.; Snurr, R. Q. *Langmuir* **2008**, *24*, 8592–8598.
(8) Li, K. H.; Olsan, D. H.; Lee, J. Y.; Bi, W. H.; Wu, K.; Yuen, T.; Xu, Q.; Li, J. *Adv. Funct. Mat.* **2008**, *18*, 2205–2214.
(9) Li, Y.; Yang, R. T. *Langmuir* **2007**, *23*, 12937–12944.
(10) Min Wang, Q.; Shen, D.; Bülow, M.; Ling Lau, M.; Deng, S.; Fitch, F. R.; Lemcoff, N. O.; Semanscin, J. *Micro. Meso. Mater.* **2002**, *55*, 217–230.
(11) Seo, J. S.; Whang, D.; Lee, H.; Jun, S. I.; Oh, J.; Jeon, Y. J.; Kim, K. *Nature* **2000**, *404*, 982–986.
(12) Cho, S. H.; Ma, B. Q.; Nguyen, S. T.; Hupp, J. T.; Albrecht-Schmitt, T. E. *Chem. Commun.* **2006**, 2563–2565.
(13) Horike, S.; Dincaìoe, M.; Tamaki, K.; Long, J. R. *J. Am. Chem. Soc.* **2008**, *130*, 5854–5855.
(14) Ma, L. Q.; Abney, C.; Lin, W. B. *Chem. Soc. Rev.* **2009**, *38*, 1248–1256.
(15) Perles, J.; Iglesias, M.; Martin-Luengo, M. A.; Monge, M. A.; Ruiz-Valero, C.; Snejko, N. *Chem. Mater.* **2005**, *17*, 5837–5842.
(16) Wu, C. D.; Lin, W. B. *Angew. Chem., Int. Ed.* **2007**, *46*, 1075–1078.
(17) Li, H.; Eddaoudi, M.; O'Keeffe, M.; Yaghi, O. M. *Nature* **1999**, *402*, 276–279.
(18) Hasegawa, S.; Horike, S.; Matsuda, R.; Furukawa, S.; Mochizuki, K.; Kinoshita, Y.; Kitagawa, S. *J. Am. Chem. Soc.* **2007**, *129*, 2607–2614.
(19) Hwang, Y. K.; Hong, D.-Y.; Chang, J.-S.; Jhung, S. H.; Seo, Y.-K.; Kim, J.; Vimont, A.; Daturi, M.; Serre, C.; Férey, G. *Angew. Chem., Int. Ed.* **2008**, *47*, 4144–4148.
(20) Yamada, T.; Kitagawa, H. *J. Am. Chem. Soc.* **2009**, *131*, 6312–6313.
(21) Halder, G. J.; Kepert, C. J. *J. Am. Chem. Soc.* **2005**, *127*, 7891–7900.
(22) Horcajada, P.; Serre, C.; Maurin, G.; Ramsahye, N. A.; Balas, F.; Vallet-Regi, M.; Sebban, M.; Taulelle, F.; Ferey, G. *J. Am. Chem. Soc.* **2008**, *130*, 6774–6780.

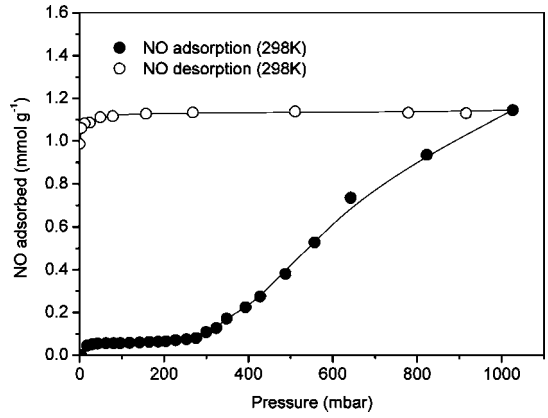

Figure 1. NO adsorption (closed symbols) and desorption (open symbols) isotherms for dehydrated Cu-SIP-3 showing the large hysteresis.

Recent work has reported the synthesis of one of these flexible so-called "third-generation" frameworks, a copper 5-sulfoisophthalate MOF called Cu-SIP-3 ($Cu_2(OH)(C_8H_3O_7S)(H_2O)\cdot 2H_2O$) with selectivity in its gas adsorption properties achieved via externally stimulated structural flexibility.[23] This work has demonstrated the low pressure selectivity of Cu-SIP-3 toward the small molecules nitric oxide (NO) and water via a coordination-driven gating mechanism. The material undergoes a structural transformation on dehydration, involving the breaking of several bonds in the low-temperature structure, driven by the change in metal coordination on the loss of coordinated water. The transformation can be reversed by exposure to water to reinstate the original metal coordination. The dehydrated material can be considered nonporous; small molecules H_2, N_2, CO_2, CO, N_2O, and CH_4 show no uptake up to pressures of 10 bar. At very low pressures (<275 mbar), exposure to nitric oxide results in similar behavior. However, on exposure to a minimum gate-opening pressure of NO (~275 mbar) the material uptakes 0.88 NO molecules per formula unit (at 1 bar), equating to 1.1 mmol g^{-1} of material at 293 K. The NO adsorption isotherm is shown in Figure 1. Such behavior is unprecedented, and the material can be considered ultraselective in its gas adsorption properties. The material shows a significant hysteresis with NO on removal of the gas pressure (Figure 1), indicating a strong interaction between the framework structure and the gas, which is likely to be a chemisorption interaction with the metal. The unique properties of this material can be attributed to the coordination flexibility of the structure, imparted by the use of a linker with the potential for both strong and weak ligand interactions. The two carboxylate functionalities on the 5-sulfoisophthalate ligand bind relatively strongly to the metals holding the structure together, while chemistry can take place at the weaker sulfonate−metal bonds, enabling the reversible chemical transformations.

In this paper, we use single-crystal X-ray diffraction to follow the changes in structure as Cu-SIP-3 is heated through the phase transition temperature and on exposure to 1 bar of NO gas. Elucidation of the mechanism of transformation, both on dehydrating the material and addition of guest molecules, is of great interest; understanding the structural reasons behind the selectivity of this material to NO could lead to the design of other materials for selective binding of NO and other gases. NO is a very important biological signaling molecule, and its exogenous administration from storage materials is of great interest for vasodilatory, antithrombotic, and wound-healing applications. NO released from other framework materials has shown the expected biological behavior,[3,24−26] and the controlled nature of NO release from this material makes it a good candidate for such an application. Release of the NO stored in Cu-SIP-3 is achieved by exposing the sample to water vapor, reforming the hydrated phase, a process similar to that of other NO-delivery MOF materials.[24,26]

In situ diffraction studies on metal−organic frameworks transitions are relatively rare. Variable-temperature powder diffraction data are commonly used in MOF materials to track the changes in unit cell parameters on the application of an external stimulus such as temperature or solvent.[23,27−31] Studies on single crystals mostly relate to changes of metal coordination or framework flexibilities on removal of solvent, or inclusion of other guest molecules. There are several reports of single-crystal to single-crystal reactions studied by diffraction reporting the changes of structure on exposure to different solvent conditions.[21,27,30,32−36] Fewer studies have been done to characterize transformations which involve significant coordination changes and large atomic movements, due to the problems associated with retaining crystallinity when there is significant movement in the crystal. Herein we report an in situ single-crystal analysis to examine the mechanism of transformation in the framework Cu-SIP-3, when both thermal and gaseous stimuli are used to induce major coordination changes in the framework. The results show that Bragg diffraction is lost as the crystal undergoes the phase transition on dehydration but is regained once the transition is complete. A similar loss of Bragg diffraction is seen on exposure to low pressures of NO.

Experimental Section

Synthesis and Crystal Structure of Cu-SIP-3·3H$_2$O. Single crystals of Cu-SIP-3 MOF were synthesized using the method outlined by Xiao et al.[23] using hydrothermal synthesis. $Cu(NO_3)_2\cdot H_2O$ (Alfa Aesar 98%, 2.42 g) and 5-sulfoisophthalic acid sodium salt (NaH_2SIP, Aldrich, 95%, 2.68 g) were dissolved in a 12 mL 50:50 EtOH−H_2O solution and heated in a 50 mL Teflon-lined autoclave at 383 K for 5 days. Crystals were cleaned

(23) Xiao, B.; Byrne, P. J.; Wheatley, P. S.; Wragg, D. S.; Zhao, X.; Fletcher, A. J.; Thomas, K. M.; Peters, L.; Evans, J, S. O.; Warren, J. E.; Zhou, W.; Morris, R. E. *Nature Chem.* **2009**, *1*, 289–294.

(24) (a) McKinlay, A. C.; Xiao, B.; Wragg, D. S.; Wheatley, P. S.; Megson, I. L.; Morris, R. E. *J. Am. Chem. Soc.* **2008**, *130*, 10440–10444. (b) Xiao, B.; Wheatley, P. S.; Zhao, X. B.; Fletcher, A. J.; Fox, S.; Rossi, A. G.; Megson, I. L.; Bordiga, S.; Regli, L.; Thomas, K. M.; Morris, R. E. *J. Am. Chem. Soc.* **2007**, *129*, 1203–1209.

(25) Mowbray, M.; Tan, X. J.; Wheatley, P. S.; Rossi, A. G.; Morris, R. E.; Weller, R. B. *J. Invest. Derm.* **2008**, *128*, 2546–2546.

(26) Wheatley, P. S.; Butler, A. R.; Crane, M. S.; Fox, S.; Xiao, B.; Rossi, A. G.; Megson, I. L.; Morris, R. E. *J. Am. Chem. Soc.* **2006**, *128*, 502–509.

(27) Halder, G. J.; Park, H.; Funk, R. J.; Chapman, K. W.; Engerer, L. K.; Geiser, U.; Schlueter, J. A. *Cryst. Growth Des.* **2009**, *9*, 3609–3614.

(28) Kubota, Y.; Takata, M.; Matsuda, R.; Kitaura, R.; Kitagawa, S.; Kobayashi, T. C. *Angew. Chem., Int. Ed.* **2006**, *45*, 4932–4936.

(29) Ghosh, Sujit K.; Zhang, J.-P.; Kitagawa, S. *Angew. Chem., Int. Ed.* **2007**, *46*, 7965–7968.

(30) Zhang, J.-P.; Lin, Y.-Y.; Zhang, W.-X.; Chen, X.-M. *J. Am. Chem. Soc.* **2005**, *127*, 14162–14163.

(31) Dietzel, P. D. C.; Johnsen, R. E.; Blom, R.; Fjellvag, H. *Chem.—Eur. J.* **2008**, *14*, 2389–2397.

(32) Kawano, M.; Fujita, M. *Coord. Chem. Rev.* **2007**, *251*, 2592–2605.

(33) Dietzel, P. D. C.; Morita, Y.; Blom, R.; Fjellvag, H. *Angew. Chem., Int. Ed.* **2005**, *44*, 6354–6358.

(34) Halder, G. J.; Kepert, C. J. *Aust. J. Chem.* **2006**, *59*, 597–604.

(35) Zhang, Y. X.; Chen, B. L.; Fronczek, F. R.; Maverick, A. W. *Inorg. Chem.* **2008**, *47*, 4433–4435.

(36) Suh, M. P.; Ko, J. W.; Choi, H. J. *J. Am. Chem. Soc.* **2002**, *124*, 10976–10977.

Table 1. Selected Crystal Data and Refinement Details for Hydrated Cu-SIP-3 (150 K), Dehydrated Cu-SIP-3 (500 K), and Rehydrated Cu-SIP-3 (293 K)

T/K	150	500	293 (rehydrated)
formula	$Cu_2O_{11}C_8S$	$Cu_4O_{16}C_{16}S_2$	$Cu_2O_{11}C_8S$
FW/g mol^{-1}	435.26	836.64	435.26
crystal system	monoclinic	monoclinic	monoclinic
space group	$P2_1/n$	$P2_1/n$	$P2_1/n$
a/Å	7.2949(4)	13.796(2)	7.3333(14)
b/Å	18.2726(10)	19.430(4)	18.153(3)
c/Å	10.1245(6)	12.057(2)	10.1729(19)
β/deg	94.8910(10)	139.172(4)	94.379(4)
V/Å^3	1344.65(13)	2112.9(16)	1350.3(4)
Z	8	8	8
ρ_{calc}/Mg m^{-3}	1.624	2.428	1.617
μ/mm^{-1}	1.81	8.92	1.80
data/restraints/parameters	4033/6/199	3412/6/343	3925/6/199
R(F) (I > 2σ(I))/%	0.0371	0.0478	0.076
R(F) (all)/%	0.0394	0.0769	0.2012
*R*w(F2) (*I* > 2σ(*I*))/%	0.1110	0.1223	0.1838
*R*w(F2) (all)/%	0.1129	0.1486	0.187
GoF	1.03	0.873	1.21

by sonication in 100 mL of EtOH−H_2O, filtered, and dried in air. An aqua-blue crystalline solid was obtained: $Cu_2(OH)(C_8H_3O_7S)(H_2O)\cdot 2H_2O$ (Cu-SIP-3).

X-ray Crystallography. Variable-temperature single-crystal X-ray diffraction data sets were collected by mounting a crystal on a glass fiber using the minimum quantity of glue in order to allow maximum maneuverability of the crystal during the structural transition and high-temperature annealing. Data were collected at Station 11.3.1 of the Advanced Light Source, Lawrence Berkeley National Laboratory, using a wavelength of $\lambda = 0.7749$ Å. A Bruker AXS APEXII diffractometer was used for data collection, and the corresponding Bruker AXS APEXII software was used during data collection and reduction. Variation in crystal temperature was achieved via the cryostream with a ramp rate of 15 K h^{-1}. The crystal temperature quoted in the subsequent data is the average cryostream temperature over the time period of data collection. Variable-temperature runs were collected using continuous shells over a 12 h period. These runs were then integrated and corrected for adsorption using the SADABS program.[37] Structures were solved using direct methods using the program SIR-97[38] and then refined on F^2 using SHELXTL-97[39] software. Non-hydrogen atoms were refined anisotropically for all structures. Hydrogen atoms were fixed based on idealized coordinates and were refined with values of U_{iso} set to 1.5 times that of the carrier atom. Full crystallographic parameters for the final refinements of selected structures are given in Table 1. See the Supporting Information for data in CIF format.

In situ gas loading experiments were performed using an environmental gas cell goniometer head.[40] The crystal was fixed on a glass fiber and secured using a minimum amount of glue, taking care not to leave any glue on exposed crystal faces. The crystal was held under vacuum and heated in the gas cell overnight to remove all solvent molecules from the structure and to anneal the crystal in the high-temperature regime. The crystal was cooled to room temperature, and a data set was collected to confirm the structural transition had taken place. Due to amorphous scattering from the glass longer collection times were required to get intense diffraction peaks while using the cell, typically three seconds per frame. Gas was introduced to the crystal slowly by introducing small bursts of nitric oxide into the cell. After each addition, the system was allowed to equilibrate and enough data collected to enable the unit cell to be indexed.

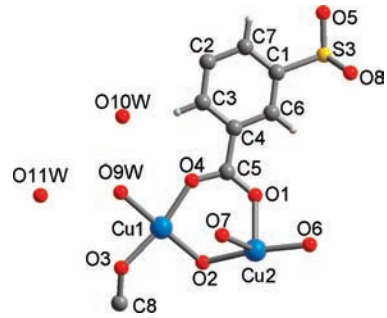

Figure 2. Asymmetric unit and numbering scheme for the low-temperature (hydrated) structure of Cu-SIP-3.

Results and Discussion

Variable-Temperature Diffraction Experiments. The low-temperature structure of Cu-SIP-3 MOF was reported by Xiao et. al.[23] The structure is formed of secondary building units based on a tetramer of Cu ions, linked by two three-coordinate hydroxyl groups. The copper tetramers are linked into layers by 5-sulfoisophthalate linkers, which are further connected into a three-dimensional network by the coordination of the sulfonate group to a cluster in another layer. In the low-temperature regime, only two of the three sulfonate oxygens are utilized in framework bonding; the third is uncoordinated and points into the space between copper clusters. The asymmetric unit (Figure 2) contains three water molecules; two (O10w, O11w) are held by hydrogen bonding in the channels defined by the framework, and one molecule (O9w) is coordinated to a copper in the tetramer.

X-ray diffraction data were collected over a range of 150−500 K. Refinements against data collected in the temperature range 150−365 K yielded the hydrated Cu-SIP-3 structure. Above 365 K, Bragg scattering became increasingly sparse and diffraction peaks distorted significantly so that their maxima could not be located precisely, meaning that the unit cell could not be determined. In the temperature range 370−405 K, no Bragg peaks could be observed in the diffraction pattern indicating loss of long-range order in the crystal, and a corresponding increase in the diffuse scattering from the crystal was observed. At temperatures higher than 405 K, Bragg diffraction reappeared and discrete diffraction spots became discernible in the pattern. Above 430 K, the data showed a highly crystalline material once more whose unit cell and crystal structure could be determined using the standard methods, and refinement yielded the dehydrated Cu-SIP-3 structure.[23] Frames of diffraction data at three different temperatures (300, 390, and 465 K) are shown in Figure 3, illustrating the sharp diffraction spots above and below the transition temperature but only broad, diffuse scattering at 390 K.

Data above 430 K solved as the dehydrated structure described by Xiao et al.[23] In this high-temperature structure, all three water molecules in the asymmetric unit of the low-temperature structure are absent. Of particular importance is the loss of the coordinated water molecule that necessitates coordination changes; the vacant site on the copper molecule is coordinated by the third sulfonate ligand oxygen (O5) which, in the low-temperature regime is uncoordinated. In order for this coordination change to take place several other coordination changes are necessary. This leads to reduction of the symmetry

(37) Sheldrick, G. M. University of Gottingen, Germany, 1996.
(38) Altomare, A.; Burla, M. C.; Camalli, M.; Cascarano, G. L.; Giacovazzo, C.; Guagliardi, A.; Moliterni, A. G. G.; Polidori, G.; Spagna, R. *J. Appl. Crystallogr.* **1999**, *32*, 115–119.
(39) Sheldrick, G. M. University of Göttingen, Germany, 1997.
(40) Warren, J. E.; Pritchard, R. G.; Abram, D.; Davies, H. M.; Savarese, T. L.; Cash, R. J.; Raithby, P. R.; Morris, R.; Jones, R. H.; Teat, S. J. *J. Appl. Crystallogr.* **2009**, *42*, 457–460.

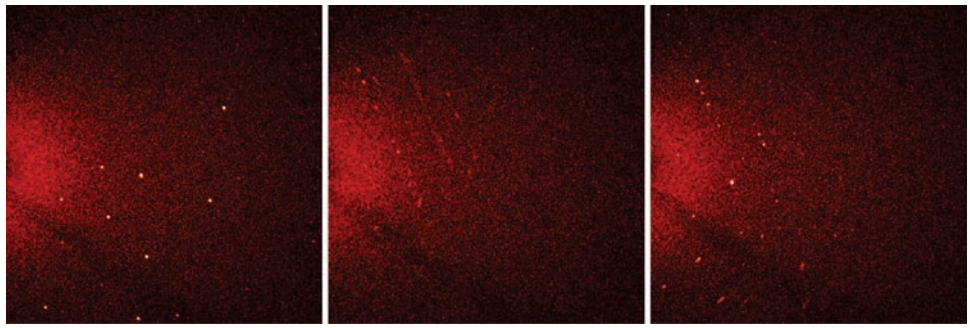

Figure 3. Snapshots of diffraction frames from variable-temperature single-crystal experiments, with the same ω value shown for each temperature. $T =$ 300 K: low-temperature structure obtained (left). $T = 390$ K: no structure obtained (middle). $T = 465$ K: high-temperature structure obtained (right).

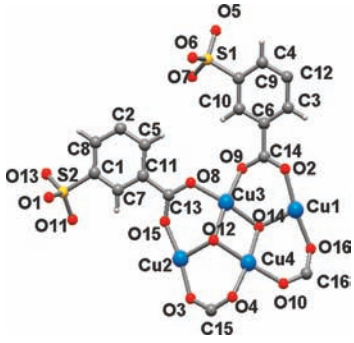

Figure 4. Asymmetric unit of the high-temperature structure of CU-SIP-3.

of the tetramer, leaving one four-, two five-, and three six-coordinated Cu ions, doubling the size of the asymmetric unit (Figure 4). Figure 5 shows the overall changes in the structure on heating.

This structural transformation represents a single-crystal to single-crystal transformation of the material, as confirmed by the similar orientation matrices of the crystal on the diffractometer in the high and low-temperature regime. The change in coordination in the copper tetramer cannot be observed using single-crystal diffraction due to the loss of long-range order associated with such a significant structural change while it is occurring. The structural transition cannot be reversed by cooling in the dry nitrogen cryostream, the material remains in the high-temperature regime at all temperatures down to at least 300 K. When exposed to moist air for a period of 3 h, the structural transition can be fully reversed and the coordinated and guest water molecules are found in full occupancy in the structure (see Table 1).

The single-crystal data are consistent with powder data reported by Xiao et al.,[23] and the changes in unit cell parameters are comparable in both techniques (figure 6). One interesting feature of the low-temperature structure is that it shows very little variation of unit cell volume with temperature and could be described as approximately a zero thermal expansion material. Of course, with the extra detail possible for single-crystal X-ray diffraction one can look more closely at the changes to the structures that occur just below the phase transition temperature.

It is possible to monitor the partial loss of guest solvent from the material between 150 and 370 K by allowing the occupancy of the three water molecules to refine freely. The occupancy of O9W, the water molecule coordinated to the copper, does not change in these temperatures. The occupancy of O11W begins to decrease in data sets of $T = 270$ K and above, and in the highest solvable data of the low-temperature structure, the water occupancy is reduced to 0.497(6). The occupancy of the other solvent molecule, O10W, remains at 1.0 until a higher temperature (~300 K), and it decreases more slowly than for O11W. The apparent slight increase of water occupancy between 340 and 370 K is unlikely to be real as occupancy and anisotropic displacement parameters (ADPs) are correlated. It is also the case that as the Bragg reflections broaden approaching the transition temperature it becomes more difficult to accurately measure reflection intensity, and there is therefore a slight reduction in the quality of the refinement in this region. Both these effects lead to a significant increase in errors on the occupancy near the transition temperature (Figure 7). When calculated from crystallographic data, assuming only the occupancy of the water changes throughout the dehydration process, the mass loss with temperature fits well with the TGA reported in reference.[23]

There is a sizable difference in occupancy between the two water molecules at temperatures higher than 270 K; O11W is lost from the structure at significantly lower temperature than O10W. When considering the hydrogen bonding of these water molecules to the framework, the average of the three likely hydrogen-bonding O···O distances is almost identical for the two waters, and this information alone does not explain the difference in behavior with temperature. However, the difference may be attributed to the local environments of the atoms involved in hydrogen bonding to the two solvent molecules. Both O10W and O11W are hydrogen bonded to the coordinated water O9W. From the geometry it is likely that O10W hydrogen bonds to O6 and O8, both part of the rigid carboxylate framework. Atomic displacement parameters (Figure 8) are small for these oxygens at all temperatures (see below), meaning the hydrogen-bonding framework of O10w is relatively stable and unperturbed by heating. In comparison, O11W likely hydrogen bonds to uncoordinated sulfonate oxygen, O5, and carboxylate oxygen, O1. O1 has broadly similar changes in ADP with temperature (Figure 8) to O6 and O8. However, the uncoordinated sulfonate O5 is considerably more susceptible to change with temperature. Its displacement parameters increase more with increasing temperature than any other oxygen in the structure. U_1, the largest magnitude of the principal mean square displacement, equating to the longest axis of an atom's thermal ellipsoid, shows marked increase with temperature (note the principal mean square displacements U_1, U_2, and U_3 are the terms from the *diagonalized* anisotropic displacement parameter tensor and are not the same as the U_{11}, U_{22}, or U_{33}). Similarly, U_{eq}, the radius of a sphere with identical volume to the ellipsoid defined by U_1, U_2, and U_3, for this atom shows an increase with temperature, with both parameters showing abrupt increases above 270 K. This is likely to relate to two aspects of the

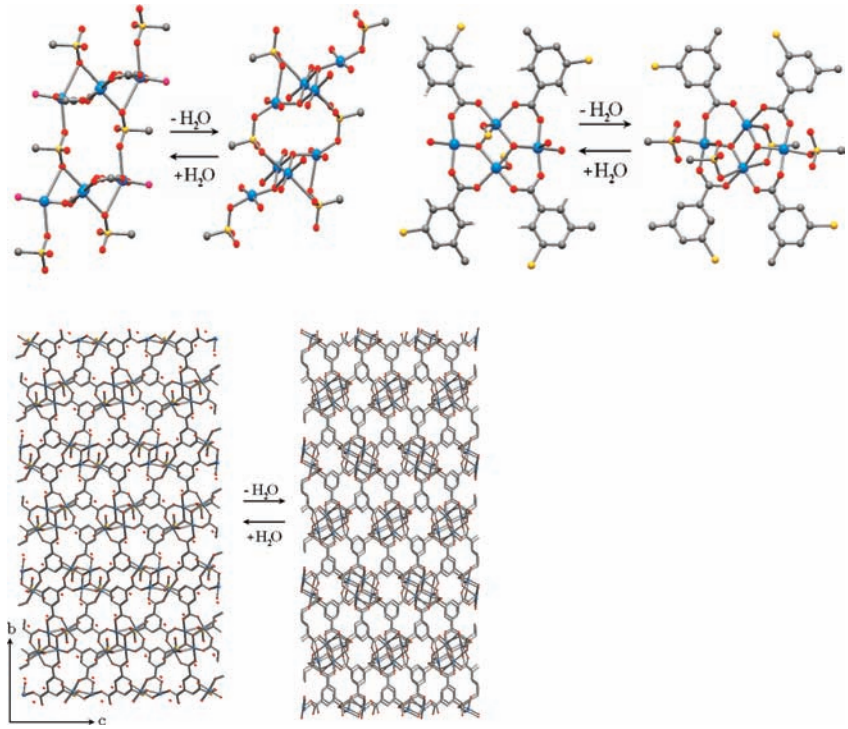

Figure 5. (a) Chains of copper tetramers in the low-temperature (left) and high-temperature (right) structures. (b) Copper tetramers in the low-temperature (left) and high-temperature (right) structures. (c) Layers in the low-temperature (left) and high-temperature (right) structures.

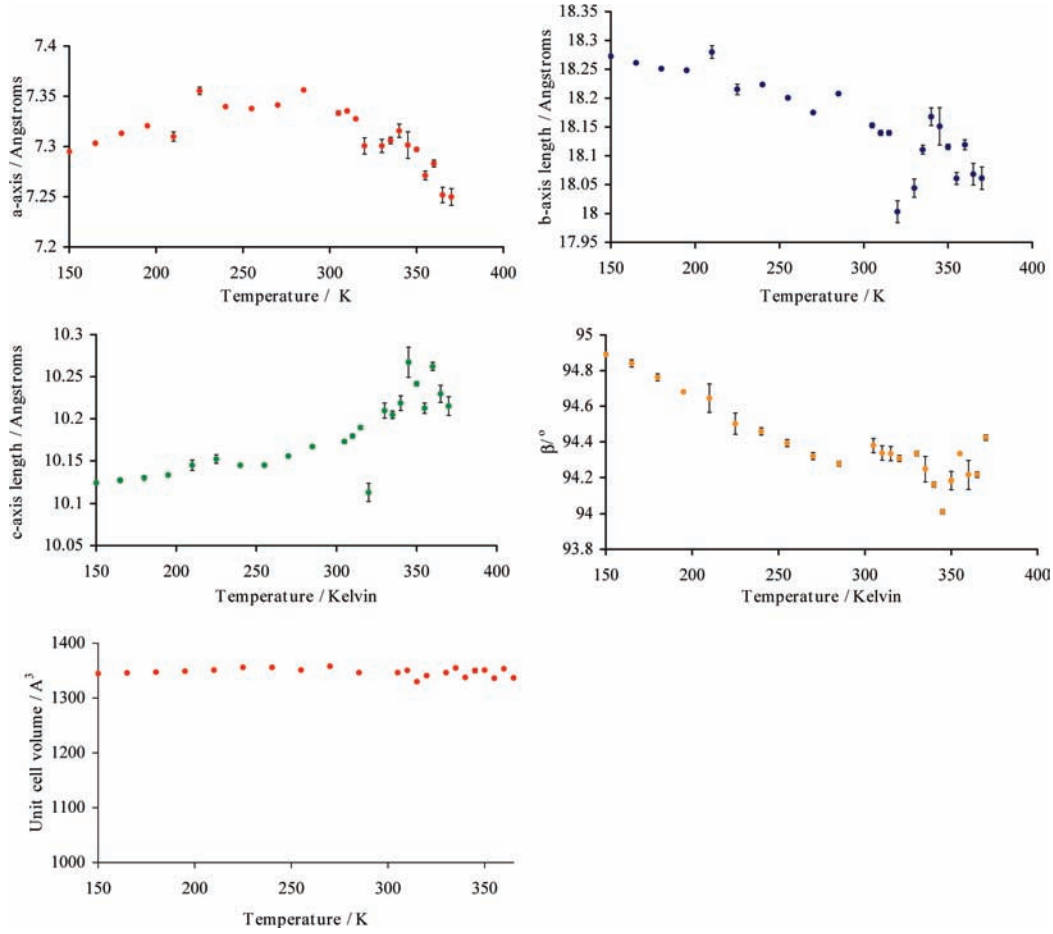

Figure 6. Change of unit cell parameters for the hydrated structure for temperatures up to the loss of Bragg diffraction. Error bars are shown on all graphs (some have small magnitude therefore are not visible).

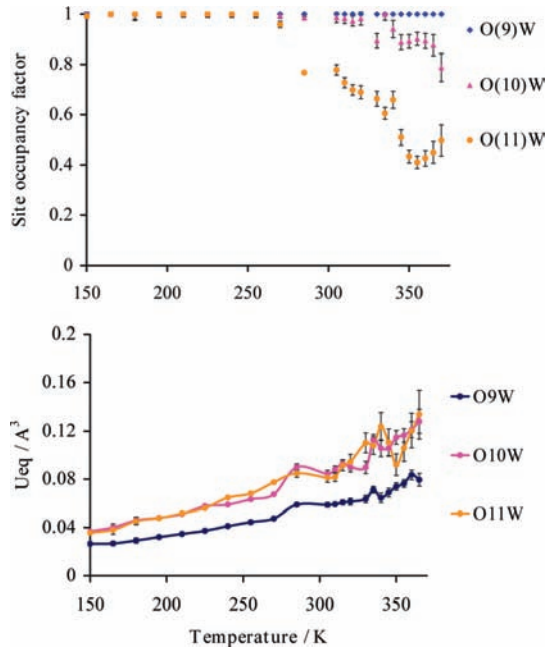

Figure 7. Change in the site occupancies with temperature. Bottom chart shows the variation of U_{eq} with temperature, correlated with the apparent rise in occupancy of O11W at temperatures above 350 K.

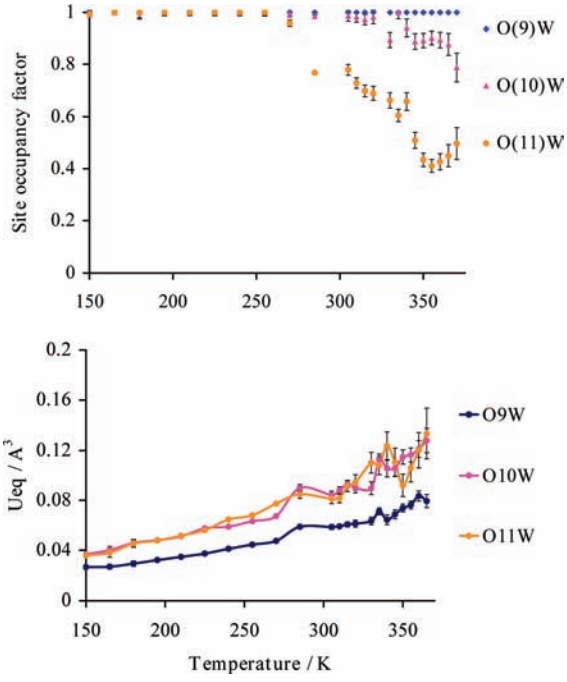

Figure 8. Variation in thermal parameters U_{eq} (the equivalent isotropic atomic displacement) and U_1 (the longest means square atomic displacement) with temperature. An increase in thermal parameters with temperature is expected due to the increased energy and enhanced vibration. The large increase of the value of ADPs for O5 is significant as movement of this atom is integral to the structural transformation of the material.

structure. First, the increase in temperature leads to greater atomic vibrations, heightened for this atom by the absence of strong framework bonding which limits movement of many of the other atoms. It is likely therefore that the hydrogen bonding for O5···O11W is more easily perturbed with temperature and leads to O11W being held less strongly in the channels than O10W. The loss of O10W from the framework will lead to loss of hydrogen-bonding interaction of O5 and, hence, further increase the potential of this atom for movement. Second, heating the crystal can been seen to add defects to the structure; as water leaves the framework, it does so one unit cell at a time, and the loss could change the geometry of O5 slightly, while other unit cells stay in their original geometry. Diffraction methods monitor the average position of an atom in the structure; in this case, the average observed by diffraction is a combination of the two geometries, evident as a very large anisotropic displacement parameter.

Comparison of anisotropic displacement parameters for the oxygen atoms in the low-temperature structure found that vibrations in the model structure at 150 K are low at all temperatures. With increasing temperature, all thermal parameters show an increase (Figure 7). Marked increase occurred in all data sets around 270 K, concurrent with the loss of water molecule O10W as previously described.

The decrease in site occupancy of O10W and the large increase in the atomic displacement parameters appear to be concurrent at 270 K. It is likely that there is some correlation between the data. It cannot be determined from this data whether the loss of water in the structure leads to the large thermal parameters seen for O5 or whether significant vibration of O5 leads to disruption of the hydrogen bonding of O11W and, therefore, the premature loss of this molecule from the structure.

O9W is found in full occupancy throughout the low-temperature refinements but is completely absent in the high-temperature structure. It is not possible to observe the loss of this water from the structure using the diffraction data; at all temperatures the occupancy of O9W remains 1.0. Instead, the molecule must be lost in the temperature range where no structure is obtained. This suggests that as soon as the molecule containing O9W begins to be lost from the structure, the atomic rearrangement takes place. Unit cells with coordinated water still present are significantly different from those without the coordinated water. Initially, when very few coordinated water molecules are lost this is probably equivalent to having a small number of "defects" in the structure, long-range order is retained on average. As more and more coordinated water molecules are lost, the concentration of these "defects" increases until there is necessarily a loss of long-range order in the structure. The order only reappears when the majority of the coordinated water is lost and the material can be regarded as having predominantly the high temperature, dehydrated structure. The loss of this molecule from the crystal induces significant structural change in parts of the crystal which destroys the long-range order, unsurprising given the large atomic movements necessary to fill the residual vacant coordination site.

In Situ NO Loading Experiments. In addition to the phase transformation on dehydration, Cu-SIP-3 also has some extremely unusual and highly selective adsorption behavior toward NO. Previous work suggests that this behavior occurs because of a coordination-driven gating mechanism, where it is coordination of the NO to the metal site that opens the gate.[23] To probe this process, a single crystal of Cu-SIP-3 was heated to 500 K to remove coordinated water while being kept away from moisture in an environmental gas cell and cooled to room temperature. Data collection confirmed that this single crystal had transformed to the high-temperature structure described above. Addition of low pressures (<275 mbar) of NO resulted in no change to the structure and the X-ray diffraction data indexed as the high-temperature structure. This is consistent with the adsorption isotherm shown in Figure 1, where no adsorption is known to take place. However, above the gate opening

pressure of 275 mbar NO (data taken at 340 mbar NO), there was immediate loss of Bragg scattering from the crystal, and only diffuse scattering remained. This behavior is consistent with the coordination-driven gating mechanism previously described. It is postulated that above the gate opening pressure long-range order is lost in the material due to coordination of the NO to copper atoms of some tetramers while others remain uncoordinated by NO, losing long-range order and so the conditions for Bragg diffraction. This can explain why it is only the strongly coordinating NO that can be adsorbed by this material. Given the reappearance of Bragg scattering at high temperatures in the dehydration experiment described above, one might expect that at high enough pressures of NO the long-range order would return to the material and single-crystal X-ray diffraction would reveal the structure of the Cu-SIP-3 NO adduct when all possible Cu tetramers were coordinated to the NO. Unfortunately, given the toxic nature of NO, the current experimental setup is limited to working at relatively low pressure (<1 bar) of NO, and so the situation where there is reappearance of Bragg scattering could not be reached. Our future experiments will involve a redesigned cell to see whether prolonged exposure to NO can lead to full structural transformation of the crystal and reappearance of the Bragg scattering to confirm whether the structure of the NO adduct can be obtained.

Conclusions

This work has demonstrated the versatility of the Cu-SIP-3 framework toward thermally activated single-crystal to single-crystal transformations; despite significant movement of the atoms in the structure during the transformation, crystallinity is maintained due to the rigid carboxylate framework. The structural transition can be reversed in full by exposure of the system to moisture with the retention of crystallinity. Addition of NO into the structure at pressures below the gating-pressure previously reported by Xiao et al. results in no change to the crystal structure. At a higher pressure of nitric oxide, Bragg diffraction is lost from the crystal and not regained.

It has been shown that single-crystal X-ray diffraction can give important information about the thermally induced structural changes in a third-generation metal−organic framework material by the comparison of data sets collected with variable temperature. It is clear that significant structural movement in this material commences around 270 K when water loss from the framework is accompanied by a stark increase in movement of all atoms, though most particularly of the uncoordinated sulfonate oxygen atom, O5. It is not possible to observe the change in coordination of the copper tetramer through diffraction methods due to the large atomic movements involved in the transition, destroying the necessary long-range crystallinity.

Acknowledgment. The Advanced Light Source is supported by the Director, Office of Science, Office of Basic Energy Sciences, of the U.S. Department of Energy under Contract No. DE-AC02-05CH11231. We thank the GEMI fund and the EPSRC for funding. R.E.M. is a Royal Society Wolfson Merit Award Holder

Supporting Information Available: Crystallographic information files for all structure determinations. This material is available free of charge via the Internet at http://pubs.acs.org.

JA910600B